PHYSICAL REVIEW B VOLUME 17, NUMBER 4 15 FEBRUARY 1978

Improved extended-x-ray-absorption fine-structure (EXAFS) studies applied to the investigation of Cu-O, Cu-N, and Cu-Br bond lengths

G. Martens, P. Rabe, N. Schwentner, and A. Werner
Institut für Experimentalphysik der Universität Kiel, Kiel, Germany
(Received 28 June 1977)

Extended-x-ray-absorption fine-structure spectra in the region of the Cu K edge are presented for Cu, CuO, Cu_2O, $CuSO_4$, $CuSO_4 \cdot 5H_2O$, $Cu(OH)_2$, $Cu(NO_3) \cdot 3H_2O$, $[Cu(NH_3)_4]^{2+}$, and $CuBr_2$. By the usual Fourier-analysis method, bond lengths for Cu-O, Cu-N, and Cu-Br are determined. Further, a back-transformation into real space is used which allows us to check the consistency of the evaluation for the whole energy range investigated. The advantages of this evaluation are: bond lengths can be taken from regions of high accuracy of the experimental data, the k dependence of the phase shifts can be checked and this presentation gives a criterion on how to fit the reference energy necessary for the energy-momentum conversion. The bond lengths determined with this method agree to within 0.02 Å with reliable x-ray diffraction data.

I. INTRODUCTION

Since the 1930's the fine structure of the absorption coefficient above the K absorption edge [extended-x-ray-absorption fine-structure (EXAFS)] has been observed. Most of the structures extending more than 50 eV above the K edge are now attributed to an interference effect at the absorbing atom caused by the electron waves outgoing from the ionized atom and the waves backscattered from the surrounding atoms. Since Stern *et al.*[1-4] proposed to use EXAFS for the determination of the structure around specific atoms, strong efforts have been made to develop EXAFS as a tool for structure analysis. Subtracting from the absorption coefficient $\mu(E)$ the K edge and a flat background one obtains the amplitude $\chi(k)$ of EXAFS:

$$\chi(k) = -\frac{1}{k}\sum_j \frac{N_j}{R_j^2} \exp(-2\sigma_j^2 - 2R_j/\lambda) \times |f_j(\pi, k)| \sin[\varphi_j(R_j, k)] \quad (1)$$

with

$$\varphi_j(R_j, k) = 2kR_j + 2\delta(k) + \arg[f_j(\pi, k)] \quad (2)$$

and

$$k = [(E - E_0)2m/\hbar^2]^{1/2} \quad (3)$$

and E the photon energy, E_0 the reference energy for the K edge, N_j the number of atoms in the jth shell, σ_j the mean displacement of the atoms, λ the electron mean free path, R_j the separation between absorbing atom and the atoms of the jth shell, $|f_j|$ the scattering amplitude and $\arg[f_j(\pi, k)]$ and δ the phase shifts of the jth shell and the absorbing atom, respectively. Modulations in $\chi(k)$ are caused by $|f_j|$ and the sine terms because the other contributions are independent on k or decrease monotonically. The backscattering amplitude $|f_j|$ is sensitive to the composition of the neighboring shells whereas the argument of the sine terms contains the structure information. For the application of EXAFS it will be decisive to find an efficient way of extracting the argument of the sine terms and further to separate R_j from the phase shifts δ and $\arg[f_j(\pi, k)]$. *Ab initio* and pseudopotential calculations,[5-7] Fourier-analysis techniques,[4,8,9] fitting procedures,[10,11] and combinations of these methods have been used with increasing success. The dominant problems of eliminating the phases, fixing the reference energy E_0 and handling the contributions of more distant shells have been stressed in all these investigations. The restricting lack of experience with different compounds of theoretically treated constituents has been stated.

In this paper we present investigations of EXAFS at the Cu K edge of the Cu-Cu, Cu-O, Cu-N, and Cu-Br bonding in a variety of compounds to study (i) the transferability of phase shifts to samples with different bonding types, (ii) to test the change of E_0 in going from metallic to insulating systems, and (iii) to test the influence of E_0 on the structure analysis. Calculations of the copper and oxygen phase shifts are available[12] and the bond lengths are known from x-ray diffraction data.

As an essential criterion for the choice of the compounds the increasing complexity of the EXAFS structure has been used. In $CuSO_4$, $CuSO_4 \cdot 5H_2O$, $Cu(OH)_2$, and $Cu(NO_3)_2 \cdot 3H_2O$, only the first oxygen shells contribute remarkably to the EXAFS structure. This simplifies the analysis. In copper oxide the analysis is complicated due to the appearance of two shells; nevertheless, a successful structure analysis by EXAFS is demonstrated. For the evaluation the Fourier-analysis method with different window functions

has been used. The results are confronted with model calculations.

II. EXPERIMENT

The continuum radiation of a 12-kW x-ray generator with a rotating Ag anode which has been monochromatized by an LiF single crystal ({200} plane) served as a structureless light source in the photon energy range from 8900 up to 9500 eV [see Fig. 1, curve *a*]. At an acceleration voltage of 30 kV and a tube current of 50–200 mA according to sample transmission counting rates of 300 000 counts/sec have been obtained above the Cu *K* edge with a NaI(Tl) scintillation detector. The spectra shown in Figs. 1, 2, and 3 have been taken with a resolution of 5 eV, a step width of 2 eV, and a statistics better than 0.1%. Before and after each transmission spectrum the spectral distribution of the incident light intensity [Fig. 1, curve *a*] has been measured for the normalization of the spectra. All data have been taken at room temperature. The energy scale has been fixed at the Cu $K\beta_{1/3}$ emission line (8905.29 eV) and the linearity has been checked versus some spurious characteristic emission lines for example the W $L\beta_4$ line (9525.2 eV) to be better than 0.5 eV in the whole energy range [see Fig. 1, curve *a*].

The samples have been prepared in different ways. For copper a thin unsupported foil of ≈3-μm thickness has been prepared by evaporation in a vacuum of better than 10^{-5} Torr. The solid compounds have been powdered and enclosed between adhesive tape to protect them from moisture and to form a uniform thin film. For $[Cu(NH_3)_4]^{2+}$ a one molar aqueous solution kept between two Mylar foils has been used.

III. EVALUATION OF THE RESULTS

The experimental absorption spectra $\mu(E)d$ are presented in Fig. 1, curve *c* and the spectra $\mu_K(E)d$ in the left column of Figs. 2 and 3 as curve *a* for each compound. The thickness of the samples has been chosen in a way to give a good contrast of the EXAFS modulation relative to the *K* edge jump but has not been determined explicitly. From the absorption spectra the EXAFS modulation $\chi(E)$ has been extracted by subtracting the monotonic background from $\mu(E)$ as is demonstrated in detail in Fig. 1 for Cu. In a first step the measured transmission spectrum Fig. 1, curve *b* has been divided by the spectral distribution of the source [Fig. 1, curve *a*] and the negative logarithm is presented as $\mu(E)d$ in Fig. 1, curve *c*. The background due to excitations of higher shells and perhaps second-order reflections has been subtracted using a Victoreen fit[13] at the low-energy side of the *K* edge [dotted curve in Fig. 1, curve *c*], yielding the absorption $\mu_K(E)d$ due to solely the Cu *K* shell. $\mu_K(E)d$ is shown as the dotted curve *d* in Fig. 1.

For a first survey all the $\mu_K(E)d$ spectra are

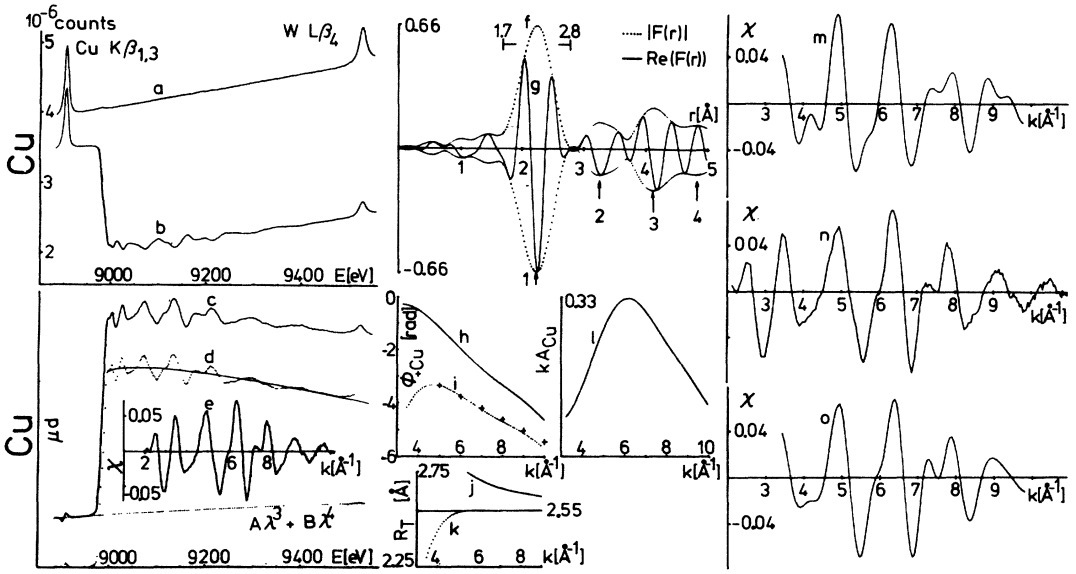

FIG. 1. Collection of EXAFS data for Cu. Left-hand column: experimental absorption spectra and EXAFS $\chi(k)$. Center column: radial structure function $|F(r)|$, $\mathrm{Re}[F(r)]$, phase shifts $\phi_{Cu}(k)$, envelope function $kA_{Cu}(k)$ of EXAFS and extracted bond lengths $R_T(k)$. Right-hand column: calculated and measured EXAFS spectra $\chi(k)$. For details see text.

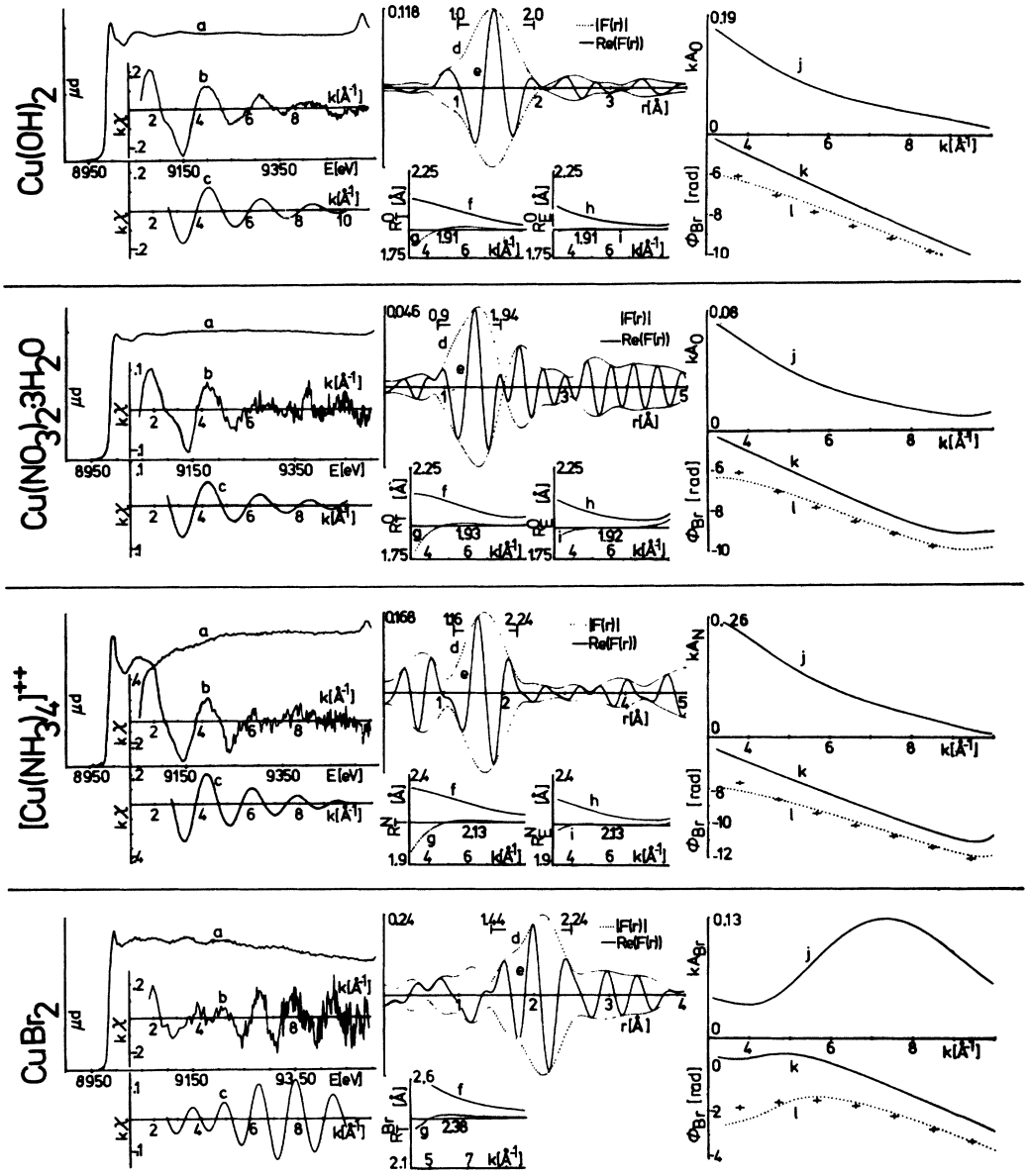

FIG. 2. Collection of EXAFS data for $Cu(OH)_2$, $Cu(NO_3)_2 \cdot 3H_2O$, $[Cu(NH_3)_4]^{++}$, and $CuBr_2$. Left-hand column: experimental absorption spectra $\mu_K d$ and EXAFS $k\chi(k)$. Center column: radial structure function $|F(r)|$, $\mathrm{Re}[F(r)]$, and extracted bond lengths $R_T(k)$, $R_E(k)$. Right-hand column: envelope function $kA(k)$ of EXAFS and phase shifts $\phi(k)$. For details see text.

treated in the same straightforward way to exclude an uncontrolled influence of the data handling. First for all the spectra the energy E_K of the K edge (half-step height) of each spectrum has been chosen as reference energy E_0 for the transformation of $\mu(E)d$ in $\mu_K(k)d$ [see Eq. (3)]. Of course this will not be the correct E_0 in general for all these compounds, but there is no consistent *a priori* way of fixing E_0. Therefore, we prefer to start with a uniform procedure. The consequences of this choice will be discussed later.

Then most of the atomic contribution was subtracted using a smooth mean value, which was determined by fitting a polynom of second degree in k to the spectra (solid curve d of Fig. 1). A spurious remainder of the atomic background has been eliminated by neglecting the first four of 256 coefficients in a Fourier analysis of the spectra before back transformation. In this way

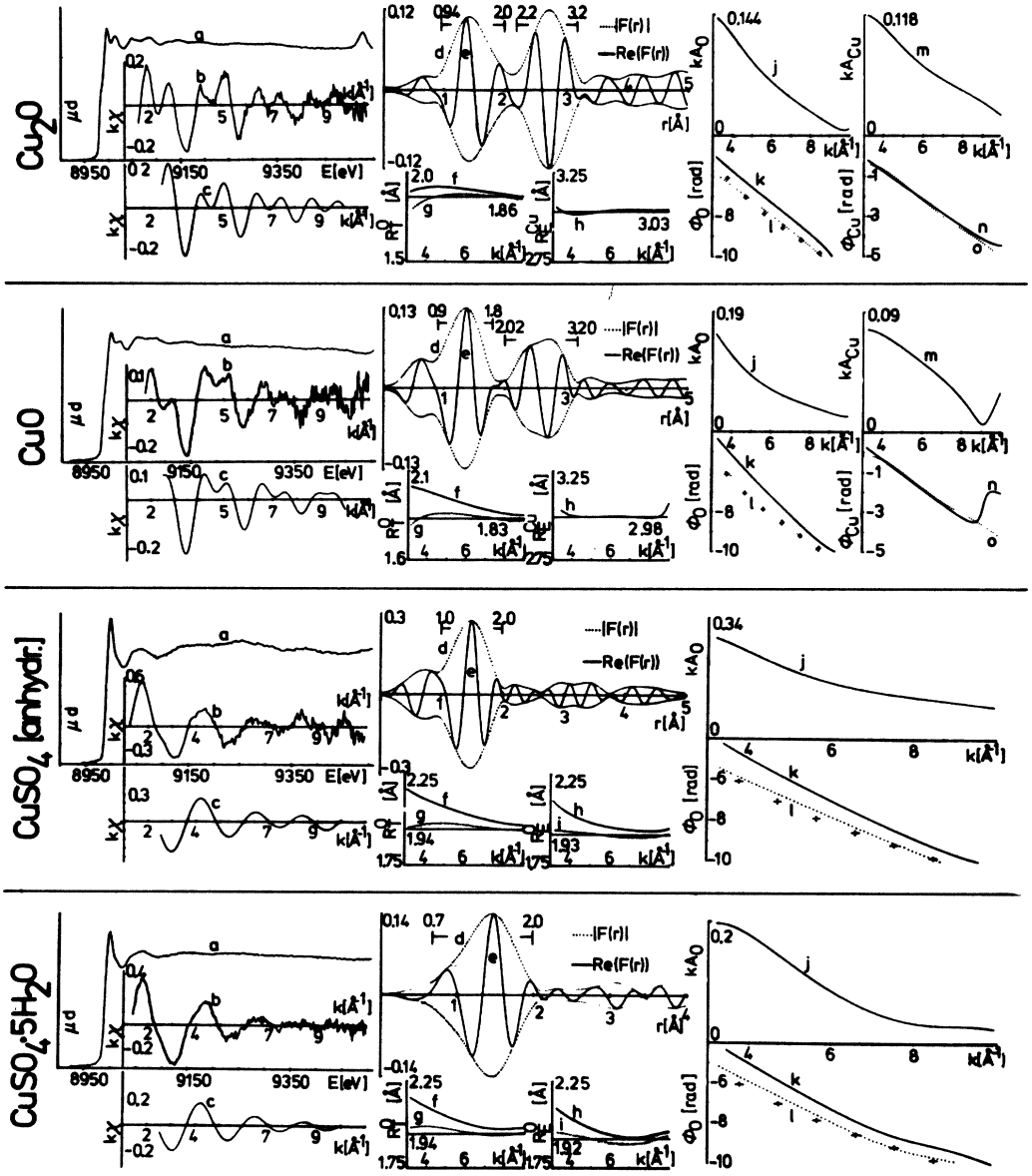

FIG. 3. Collection of EXAFS data for Cu_2O, CuO, $CuSO_4$ (anhydrous), and $CuSO_4 \cdot 5H_2O$. Left-hand column: experimental absorption spectra $\mu_K d$ and EXAFS $k\chi(k)$. Center column: radial structure function $|F(r)|$, $\mathrm{Re}[F(r)]$, and extracted bond lengths $R_T(k)$, $R_E(k)$. Right-hand column: envelope function $kA(k)$ of EXAFS and phase shifts $\chi(k)$. For details see text.

$\chi(k)\mu_0(k)d$ is obtained. To get $\chi(k)$ the atomic contribution $\mu_0(k)d$ is approximated by

$$\mu_0(k)d = \mu_K(k)d - \chi(k)\mu_0(k)d \qquad (4)$$

and thus we get $\chi(k)$ in dividing $\chi(k)\mu_0(k)d$ by Eq. (4). In Eq. (4) additional contributions to $\mu_K(k)$ like inelastic scattered electrons and many body excitations are neglected which means that we get only a lower limit for the absolute value of $\chi(k)$. Further, the envelope of $\chi(k)$ may be influenced by this approximation but for the modulation itself only minor changes are expected. Fig. 1, curve *e* and all the curves *b* in Figs. 2 and 3 show the results for $\chi(k)$ multiplied by k [except Fig. 1(e)] to increase the amplitude at high k values. In this way all the EXAFS spectra $\chi(k)$ have been obtained. These spectra are the starting point to discuss the phase shifts δ and $\arg[f_j(\pi, k)]$, the bond lengths R_j, the reference energies E_0 and the envelope functions $A_j(k)$.

In a second step a Fourier transformation from k space to R space is applied to $kF(k)\chi(k)$. Several window functions $F(k)$ (Gaussian, a convolution of Gaussian and square window, square window and cosine) have been tested with model spectra for $\chi(k)$. For all samples except Cu and $CuBr_2$ a Gaussian window has been taken which reaches $\frac{1}{10}$ of the maximum value at the nodes of $\chi(k)$ around $k = 2$ Å^{-1}. This window has been chosen because side lobes are well suppressed and the uncertain parts of the spectra at high and low k values, that means the influence of low statistics and the choice of E_0, respectively, are adequately weighted. We tolerate the broadening of structures caused by the reduction of effectively contributing k values. For Cu and $CuBr_2$ a convolution of a square and a Gaussian window has been used because in these cases $\chi(k)$ shows small amplitudes even at low k values. The real part and the magnitude (structure function) of the Fourier transform are shown in Fig. 1, curves f and g and in the second column of Figs. 2 and 3 in all curves d and e. In most of the structure functions a peak below 1 Å is observed. The position, shape, and amplitude of these maxima are rather dependent on the choice of the window function and on the details of the background subtraction. Therefore, these structures are attributed to spurious effects of the data handling.

In the following we will focus our interest on the main maxima which are indicated in Fig. 1 by arrows. The maxima are attributed to shells of atoms surrounding the absorbing copper atoms. Evidently the spectra can be ordered on the basis of the structure function in terms of increasing complexity. Compounds with only one remarkably contributing shell are collected in Fig. 2, namely, $Cu(OH)_2$, $Cu(NO_3)_2 \cdot 3H_2O$, $[Cu(NH_3)_4]^{2+}$, and $CuBr_2$ and also partly in Fig. 3, namely, $CuSO_4$ (anhydrous) and $CuSO_4 \cdot 5H_2O$. In all these compounds except $[Cu(NH_3)_4]^{2+}$ and $CuBr_2$ the central copper atom is surrounded by an octahedral distribution of nearest neighbors of oxygen atoms. The bond lengths to these atoms are partly different as listed in Table I. But according to the available x-ray diffraction data the differences of at least the first two bond lengths are less than 0.1 Å.[14-20] Due to the limited range of data in k space the maxima in R space are rather broad (≈0.3 Å) and therefore, the different Cu-O and Cu-N bond lengths are not resolved, not even in the real or imaginary part of the Fourier transform. They may be partly responsible for the width and some fine structure in the maxima. The third oxygen

TABLE I. Compilation of bond lengths from x-ray diffraction, R_C, and from Fourier transform (FT) of EXAFS: $R_A - \alpha$ peak position in the magnitude of FT; R_A, determined from $R_A - \alpha$ with α^{Cu-Cu} from pure Cu and α^{Cu-O} from Cu_2O; R_T and R_E, determined after back transformation of FT to k space using k-dependent theoretical and experimental phases, respectively. ΔE_0 differences of reference energies relative to K edge of the measured compound determined with theoretical phases.

Compound	Shell	R_C (Å)[a]	$R_A - \alpha$ (Å)	R_A (Å)	R_T (Å)	R_E (Å)	ΔE_0 (eV)
Cu_2O	O	1.84	1.41		1.86		−6
	Cu	3.02	2.72	3.04		3.03	
CuO	O_I	1.95 1.88	1.35	1.78	1.83	1.81	
	O_{II}	1.96					
	Cu_I	2.88				2.90	−12
	Cu_{II}	3.07	2.74	3.06		3.07	
$CuSO_4$	O_I	1.87 1.89	1.48	1.91	1.94	1.93	
	O_{II}	2.15 2.00					−12
	O_{III}	2.36 2.37					
$CuSO_4 \cdot 5H_2O$	O_{I-IV}	1.8–2.45	1.46	1.89	1.94	1.92	−12
$Cu(OH)_2$	O_I	1.93	1.44	1.87	1.91	1.91	
	O_{II}	1.94					−15
	O_{III}	2.63					
$Cu(NO_3)_2 \cdot 3H_2O$	O	1.9–2.0	1.56	1.99	1.93	1.92	−15
$[Cu(NH_3)_4]^{++}$	N	2.04–2.06	1.67	2.10	2.13	2.13	−15
$CuBr_2$	Br	2.40			2.38		−15
Cu	Cu_I	2.56	2.24		2.55		
	Cu_{II}	3.62	3.24	3.56		3.61	
	Cu_{III}	4.43	4.11	4.43			−16
	Cu_{IV}	5.11	4.82	5.14			

[a]References for R_C: Cu_2O (14), CuO (14,15), $CuSO_4$ (18,19), $CuSO_4 \cdot 5H_2O$ (14), $Cu(OH)_2$ (17), $Cu(NO_3)_2$ (16), $[Cu(NH_3)_4]SO_4 \cdot H_2O$ (20), $CuBr_2$ (14), Cu (15).

shells are rather far apart and not strongly occupied and the bond lengths to the following shells with strong scattering amplitudes are even larger. As is evident from the structure functions (Figs. 2 and 3) these shells do not contribute remarkably because of the damping of the outgoing electron waves. In the planar structure of $[Cu(NH_3)_4]^{2+}$ and $CuBr_2$ the absorbing copper atom is surrounded by four N or Br atoms, respectively, which cause the strong maximum in the structure function.

Now we turn to the evaluation of bond lengths. We start with a commonly used procedure. The scattering phase is approximated by a linear function in k and bond lengths R are obtained by adding the linear part α to the position of the maxima in the structure function.[4] The scattering phase for the Cu-O bond has been determined from the data of Cu_2O by a comparison of $R-\alpha$ with the known bond length R_c as is explained below. Taking the same value of $\alpha = 0.43$ Å for all Cu-O shells in the other oxygen compounds and even for the N shell in $[Cu(NH_3)_4]^{2+}$ we get values R_A for the bond lengths which are in quite good agreement with x-ray diffraction data R_c. According to Table I the differences are smaller than 0.1 Å. In Fig. 3 also the more complex spectra of Cu_2O and CuO are presented. In both compounds the central copper atom is surrounded by a planar distribution of oxygen atoms. The following shell (Cu_2O) or two shells (CuO) are formed by copper atoms. Therefore, in the copper oxides there exists a shell of nearest-neighbor oxygen atoms and also shells of next-nearest-neighbor copper atoms, which are highly occupied, not too far apart and not shielded by other atoms. The first maximum in the structure function in Fig. 3 corresponds to the Cu-O bond length and the second to the Cu-Cu bond length. The positions of the maxima are listed in Table I. The difference between the x-ray diffraction bond length and the position of the first maximum of Cu_2O yields the phase α^{Cu-O} for the Cu-O bonding which has been used above and also for CuO to extract the corresponding bond length (Table I). Further the Cu-Cu bond length R_A^{Cu-Cu} in Cu_2O and CuO has been evaluated from the maxima in the structure function by adding the phase α^{Cu-Cu} for scattering at the Cu atoms (Table I). Again there is an agreement within 0.1 Å with the x-ray diffraction data. For α^{Cu-Cu} we used our value derived from the data of pure copper as is discussed next.

The EXAFS spectrum of pure copper has been investigated for the following reasons: (i) to compare our way of data handling with the results of former investigations, (ii) to determine the term of the phase linear in k and, (iii) to treat a rather complex spectrum with several contributing shells. In the structure function of Fig. 1, curve f, 4 shells marked by arrows are identified in agreement with Ref. 4. From the positions of the maxima and with the well-known bond lengths of the shells the phase terms α^{Cu-Cu} can be derived for each shell independently. The comparison (Table I) gives a value $\alpha^{Cu-Cu} = 0.32$ Å for the first shell, which we used for the copper-oxygen compounds. For the other shells we find values between 0.29 and 0.38 Å. Within our accuracy for all shells similar phase shifts can be used. In Ref. 4 rather different phase shifts ranging from 0.14 Å for the first shell up to 0.36 Å for the fourth shell have been obtained. Bearing the concept of the transferability of phase shifts in mind we feel that rather similar phase shifts should be expected in agreement with our result. The main reason for the deviation between α^{Cu-Cu} determined by us and that of Ref. 4 is the use of different reference energies E_0, whereas the influence of the experimental spectra is of minor importance. Also the weighting of $\chi(k)$ for the different k regions by the window functions affects the scattering of the α values. If E_0 and the choice of the essential k space are decisive for the phase shifts a refined concept is necessary to treat the results of different samples. Further, there is now enough experimental[21] and theoretical[12] information available, which show that in general the phase shifts are not adequately described by a linear k dependence. For the R determination from the maxima in the structure function a linear k dependence has to be supposed, because otherwise terms of higher order in k contribute to the positions of the maxima. To avoid this problem model calculations of EXAFS spectra including a nonlinear k dependence of the phases[10,11] have been used. This method is more time consuming and less straightforward.

To utilize the advantages of both concepts we propose an extended Fourier-analysis method, which allows an arbitrary k dependence of the phases and provides a check of the quality of the evaluation in the whole k space available in the experiment: Each maximum in the structure function is back transformed separately from R space into k space. The R space which has been included in the transformation is indicated by horizontal bars in Fig. 1, curve f and the curves d of Figs. 2 and 3. After deconvolution with the inverse window function the magnitude $A_j(k)$ and the phase $\varphi_j(R_j, k)$ are derived from the real and imaginary part of the resulting EXAFS spectrum. These spectra correspond to the contribution of this shell to the original EXAFS spectra. The magnitudes of the first and in CuO_2 and CuO also for the second shells are presented in Fig. 1, curve l

and in the curves j and m of Figs. 2 and 3. According to Eq. (1) $A_j(k)$ gives

$$A_j(k) = k^{-1} |f_j(\pi, k)| (N_j/R_j^2) \times \exp(-2\sigma_j^2 k^2 - 2R_j/\lambda), \quad j = 1, 2. \tag{5}$$

Besides constant terms and the monotonic decreasing Debye-Waller factor the magnitude only contains the backscattering amplitude of the neighboring atoms. Therefore, $A_j(k)$ characterizes the species of scattering atoms. The typical behavior of the backscattering amplitude of Cu (Fig. 1, curve l), of O (for example curves j in Fig. 3), and Br (curve j of $CuBr_2$ in Fig. 2) is obvious and it is in qualitative agreement with theoretical calculations.[12] The special feature at 9 Å^{-1} in $A_2(k)$ of CuO (Fig. 3 curve m) is discussed later.

For the determination of bond lengths we use Eq. (2) and the phase $\varphi_j(R_j, k)$ obtained by the back transformation. With the theoretically calculated phase shifts from Ref. 12 for the scattering atoms O, Cu, and Br and for the absorbing atom we get

$$R_j(k) = \{\varphi_j(R_j, k) - 2\delta(k) - \arg[f_j(\pi, k)]\}/2k. \tag{6}$$

$R_1(k)$ for the first shells is shown in Fig. 1, curve j, Fig. 2, curve f and Fig. 3, curve f. The deviations of $R_1(k)$ from a constant value are due to experimental uncertainties, incorrect theoretical phase shifts, and wrong reference energies E_0. The experimentally most certain region is situated around 8 Å^{-1}. The strong increase in R to lower k values is due to an incorrect reference energy whereas at higher k values the limited statistics in the experiment plays a major role. Nevertheless, these curves show a clear trend and R values can be extracted around 8 Å^{-1} with an accuracy of ±0.05 Å. The evaluation has been further refined by fitting E_0 for the calculation of the k scale [Eq. (3)] in the back transformation in a way to get constant R_j values over a large region in k space. The result for $R_j(k)$ after this optimization is shown in the curves g in Figs. 2 and 3 and curve k of Fig. 1. Evidently these fits are quite successful and the values for the bond lengths called R_T and the differences $\Delta E_0 = E_0 - E_K$ of the reference energies and the above defined K-shell energy E_K are listed in Table I. The agreement with x-ray diffraction data is satisfactory and it is demonstrated that the bond lengths can be determined to ±0.01 Å with an inherent control of the evaluation. In a reverse procedure phase shifts have been obtained experimentally from Eq. (6) by using our R_T values and our $\varphi_j(k)$. These phase shifts $\Phi_j(k) = 2\delta(k) + \arg[f_j(\pi, k)]$ are shown in Fig. 1, curve h, Figs. 2 and curves k using the position E_K at half-step height of the K edge as reference energy E_0, i.e., $E_0 = E_K$. At moderate k values the linear term in the k dependence resembles quite well the theoretical curve but at low k values the difference is remarkable. With the reference energy E_0 fitted as explained above the experimental phase shifts $\Phi_j(k)$ (dotted curves in Figs. 2 and 3 and dotted curve in Fig. 1) nicely follow the calculated phase shifts.

To show the transferability of phase shifts the same method to determine $R(k)$ has been applied but the calculated phase shifts $2\delta(k) + \arg[f_j(\pi, k)]$ have been replaced by our $\Phi_0(k)$ (E_0 is the Cu K edge or E_0 fitted) and the results are shown as curves h and i of Figs. 2 and 3 (except CuO, Cu_2O, and $CuBr_2$) yielding the same or even more convincing $R(k)$ curves. The bond lengths are named $R_E(k)$ and are listed in Table I.

The second shell that means the Cu-Cu bond length in Cu_2O and CuO has been treated in principle in the same way but using our experimental phase shifts $\Phi_{Cu}(k)$ from copper. The reference energy E_0 has been obtained from the fit of the first shell that is the O shell (curve h in Fig. 3). The $R(k)$ curve is flat as expected and the bond length $R_E^{Cu\text{-}Cu}$ again appears in Table I.

Finally we want to mention two further aspects:

(a) For copper an EXAFS spectrum has been calculated from the x-ray diffraction bond lengths of the first 4 shells and our experimental phase shift (Fig. 1, curve h), the magnitude $A_{Cu}(k)$ (from the first shell) and reference energy E_0. This spectrum (Fig. 1, curve m) is compared with the measured EXAFS spectrum in Fig. 1, curve n. The agreement is good except for the fine structure around 4 Å^{-1}, 7.5 Å^{-1}, and 9 Å^{-1}. These discrepancies are removed if the phase shift of the fourth shell is changed by π (Fig. 1, curve o). This observation concurs with the interpretation, that the fourth shell is shaded by shells in between and that the contribution of the fourth shell includes multiple scattering.[22] It demonstrates that the experimental phase shifts allow to discuss such details. In a similar way the $\chi(k)$ spectra have been calculated from our experimental $\varphi_j(k)$ and $A_j(k)$ values for all the other compounds. The spectra are shown in Figs. 2 and 3 curves c.

(b) It remains to explain the structures in the phase and magnitude $A_{Cu}(k)$ due to the Cu-Cu bonding in CuO (Fig. 3 curves m and n). In CuO two shells of copper atoms surround the absorbing copper atom at 2.88 and 3.07 Å (Table I) giving rise to two back scattered electron waves which interfere at the absorbing atom. The minimum in $A_{Cu}(k)$ and the jump in the phase appear at k values when the envelope of the two superimposed waves reaches the first minimum. This condition is very sensitive to the difference in the bond

lengths of the two shells and enables to determine a separation of 0.19 Å with an accuray of to 0.01 Å. More details are discussed in Ref. 8.

Summary:

(1) EXAFS spectra of copper and copper compounds have been presented with statistics better than 0.1%.

(2) An improvement of the Fourier-analysis method has been shown and used to determine: (a) bond lengths with an accuracy of ≤ 0.01 Å, (b) the k dependence of phase shifts, (c) the reference energies E_0.

(3) The quality of the evaluation can be checked inherently.

(4) The transferability of phase shifts for metallic to ionic and covalent bonding and for hydrate envelopes has been demonstrated.

ACKNOWLEDGMENT

Support of the experiment by Professor R. Haensel and Dr. M. Skibowski is gratefully acknowledged.

[1]D. E. Sayers, E. A. Stern, and F. W. Lytle, Phys. Rev. Lett. 27, 1204 (1971).
[2]E. S. Stern, Phys. Rev. B 10, 3027 (1974).
[3]F. W. Lytle, D. E. Sayers, and E. A. Stern, Phys. Rev. B 11, 4825 (1975).
[4]E. A. Stern, D. E. Sayers, and F. W. Lytle, Phys. Rev. B 11, 4836 (1975).
[5]B. M. Kincaid and P. Eisenberger, Phys. Rev. Lett. 34, 1361 (1975).
[6]P. A. Lee and J. B. Pendry, Phys. Rev. B 11, 2795 (1975).
[7]P. Lagarde, Phys. Rev. B 14, 741 (1976).
[8]G. Martens, P. Rabe, N. Schwentner, and A. Werner, Phys. Rev. Lett. 39, 1411 (1977).
[9]D. E. Sayers, F. W. Lytle, M. Weissbluth, and P. Pianetta, J. Chem. Phys. 62, 2514 (1975).
[10]S. P. Cramer, T. K. Eccles, F. Kutzler, K. O. Hodgson, and S. Doniach (unpublished).
[11]R. G. Shulman, P. Eisenberger, W. E. Blumberg, and N. A. Stombauch, Proc. Natl. Acad. Sci, USA 72, 4003 (1975).
[12]P. A. Lee and G. Beni, Phys. Rev. B 15, 2862 (1977); C. A. Ashley and S. Doniach, Phys. Rev. B 11, 1279 (1975).
[13]*International Tables for X-Ray Crystallography III*, edited by K. Konsdale *et al.* (Kynoch, Birmingham, England, 1962), Sec. 3.2
[14]*Gmelin's Handbuch der anorganischen Chemie*, Teil B 1, *Cu und seine Verbindungen*, edited by E. H. E. Pietsch *et al.* (Verlag Chemie, Weinheim, Germany, 1958).
[15]R. W. G. Wyckoff, *Crystal Structures* (Interscience, New York, 1968).
[16]A. F. Wells, *Structural Inorganic Chemistry* (Oxford U.P., London, 1962).
[17]H. Jaggi and H. R. Oswald, Acta Cryst. 14, 1041 (1961).
[18]P. A. Kokkoros and P. J. Rentzeperis, Acta Cryst. 11, 361 (1958).
[19]B. Rama Rao, Acta Cryst. 14, 361 (1961).
[20]F. Mazzi, Acta Cryst. 8, 137 (1955).
[21]P. H. Citrin, P. Eisenberger, and B. M. Kincaid, Phys. Rev. Lett. 36, 1346 (1976).
[22]G. Beni, P. A. Lee, and P. M. Platzmann, Phys. Rev. B 13, 5170 (1976).